Electronic Supplementary Material (ESI) for Sustainable Energy & Fuels.

Oxalate metal organic framework-derived Ru^{3+}-doped $Co(OH)_2$ nanosheets for highly efficient hydrogen evolution reaction

Yizhong Zou,[a‡] Wen-Da Zhang,[a‡] Minghan Hu,[b] Zhe Zhang,[a] Jiangyong Liu,[c] Zhi-Guo Gu[a] and Xiaodong Yan*[a]

[a] Key Laboratory of Synthetic and Biological Colloids, Ministry of Education, School of Chemical and Material Engineering, Jiangnan University, Wuxi 214122, China

[b] Department of Materials, ETH Zürich, Zürich 8093, Switzerland

[c] School of Chemistry and Chemical Engineering, Yangzhou University, Yangzhou 225002, China

† These authors contributed equally.

E-mail: xiaodong.yan@jiangnan.edu.cn

Experimental section

Materials. Cobalt chloride hexahydrate ($CoCl_2 \cdot 6H_2O$, 99%), sodium oxalate ($Na_2C_2O_4$, 99.5%), Ruthenium chloride trihydrate ($RuCl_3 \cdot 3H_2O$, 97%), hydrochloric acid (HCl, 37.5%), ethanol (CH_3CH_2OH, 99.5%), acetone (C_3H_6O, 99.5%) were purchased from Sinopharm Chemical Reagent Co. ltd. Potassium hydroxide (KOH, 95%) were purchased from Shanghai Macklin Biochemical Co. ltd. Nickel foam (NF) with a thickness of 2 mm was purchased from Suzhou Wingrise Energy Technology Co., Ltd. Deionized water has a specific resistance of > 18.2 MΩ cm. All chemicals were purchased from commercial sources and used without further purification.

Synthesis of, Ru-CoC_2O_4-2

First, a pieces of NF (1×3 cm^2) was washed with 3 M hydrochloric acid for 10 minutes to remove the oxide layer from the surface of the NF, and then washed sequentially with ethanol, acetone, and deionized water for 10 minutes to remove the possible organic contaminants. Next, 237 mg $CoCl_2 \cdot 6H_2O$, 67 mg NaC_2O_4, and 20 mg $RuCl_3 \cdot 3H_2O$ were dissolved into 10 ml deionized water, then sonicated for 10 min to make them completely dissolved. The cleaned NF was added into the above solution, which was sealed and maintained in an oven at 120 °C for 6 h. The products were washed successively with deionized water and ethanol, and then transferred to the oven at 60 °C for drying. For the comparative study, the CoC_2O_4, Ru-CoC_2O_4-1 and Ru-CoC_2O_4-3 were produced by using different qualities of 0 mg, 10 mg and 30mg $RuCl_3$ $3H_2O$, respectively.

Synthesis of, Ru-$Co(OH)_2$-2

2.95g KOH was dissolved in 10 ml deionized water to form solution. the Ru-CoC_2O_4-2 were converted to Ru-$Co(OH)_2$-2 by placing them in above solution for 15 min, and the samples were washed successively with deionized water and ethanol. Different concentrations of ruthenium-doped cobalt hydroxide were named as $Co(OH)_2$, Ru-$Co(OH)_2$-1, Ru-$Co(OH)_2$-3.

Physical characterization

XRD characterization was performed on a Bruker D8 Venture diffractometer (Bruker Corporation, faaa USA) using a Cu-Kα radiation source (λ = 1.54178 Å) at a scan rate of 5° min^{-1}. The morphology was examined using the Hitachi S-4800 high-resolution scanning electron microscope (SEM, Hitachi ltd., Japan) and JEM-2100 high-resolution transmission electron microscope (HRTEM, JEOL ltd., Japan) equipped with energy dispersive spectroscopy (EDS) system. SEM and TEM were operated at

5 and 200 kV, respectively. XPS measurements were performed on an AXIS SUPRA, The data of all samples were calibrated by C 1s to 284.8 eV. Raman measurements were performed on a Renishaw inVia reflex Raman microscope equipped with a 785 nm laser (Renishaw, UK). *In situ* Raman data were recorded on the above-mentioned Raman microscope under controlled potentials by electrochemical workstation. The cell was made of Teflon and covered with a round quartz glass to protect the objective. Platinum wire and Hg/HgO electrode were used as counter and reference electrodes, respectively. Raman data were obtained at potentials of, 0, -0.8, -1.0, and -1.2 V vs. Hg/HgO, and the dwell time at each potential was 5 min. Inductively coupled plasma (ICP) coupled with optical emission spectrometry (OES) analysis was conducted using a PerkinElmer 8300.

Electrochemical measurement

Electrochemical measurements were performed at room temperature. A three-electrode system was used to attach to a CHI760E Electrochemical workstation (Shanghai Chenhua Instrument Co., LTD.). 1.0 mol/l KOH was used as an electrolyte. Hg/HgO electrode and carbon rod were used as reference electrode and counter electrode, respectively. The electrocatalytic performance was studied by linear sweep voltammetry (LSV). Polarization curves were obtained at a sweep rate of 5 mV/s. All polarization curves were with iR-corrected. In all measurements, the reference electrode was calibrated with respect to reversible hydrogen electrode (RHE). Electrochemical impedance spectroscopy (EIS) was performed between 0.1 Hz and 100 kHz. To measure the double layer capacitance, cyclic voltammetry (CV) curves were measured at 20, 40, 60, 80, and 100 mV s^{-1}. The electrochemical stability of the prepared Ru-$Co(OH)_2$-2 was evaluated by chronopotential measurement. All LSV curves were scanned from negative to positive at a scan rate of 10 mV s^{-1}. The potentials against the Hg/HgO electrode were converted to the RHE reference scale by: E (V vs. RHE) = E (V vs. Hg/HgO) + 0.059 × pH + 0.098.

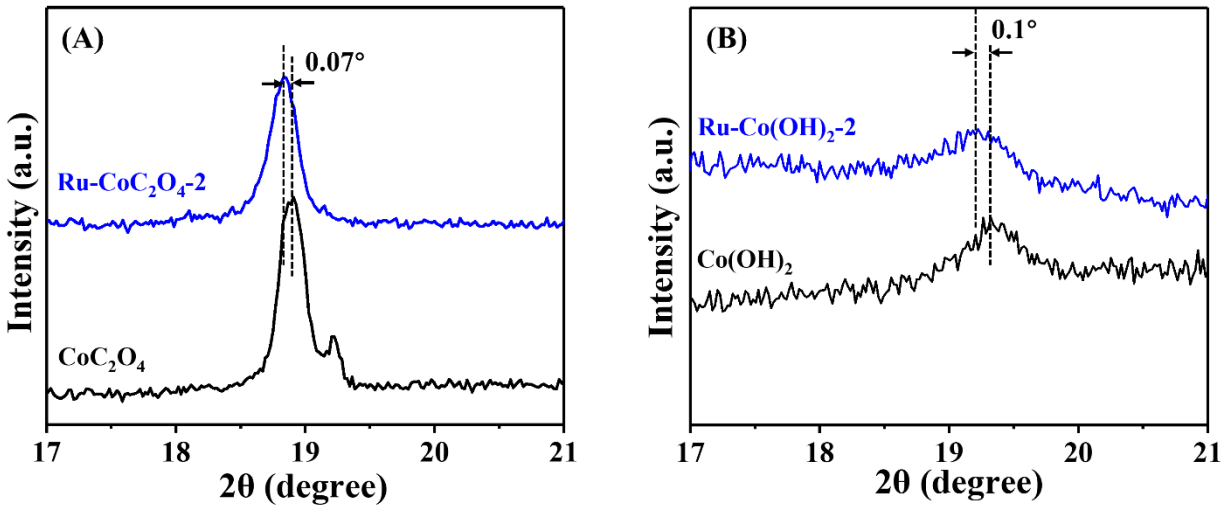

Fig. S1 Magnified XRD pattern of (A) CoC_2O_4 and Ru-CoC_2O_4-2 and (B) $Co(OH)_2$ and Ru-$Co(OH)_2$-2.

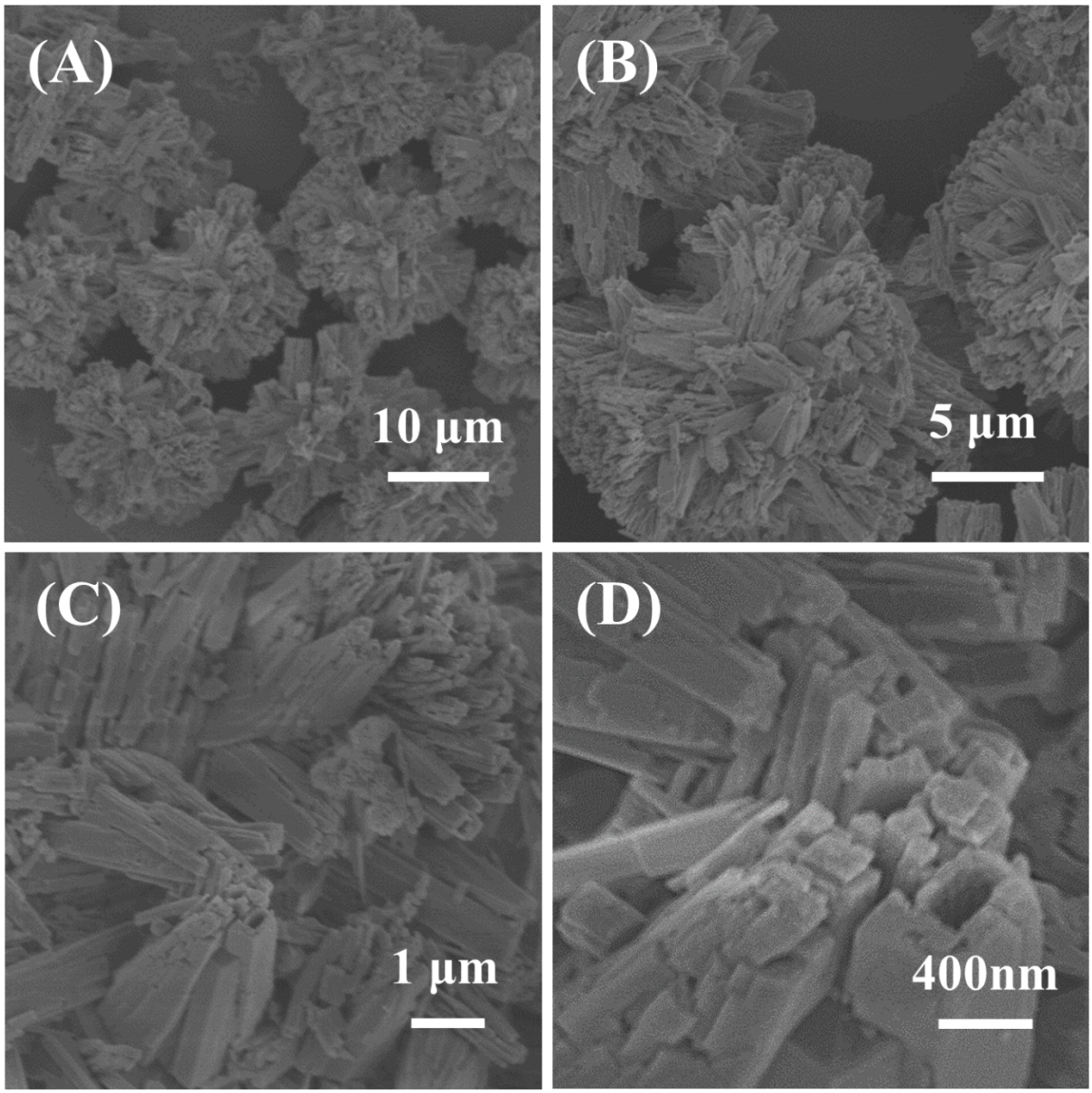

Fig. S2 SEM images of Ru-CoC_2O_4-2.

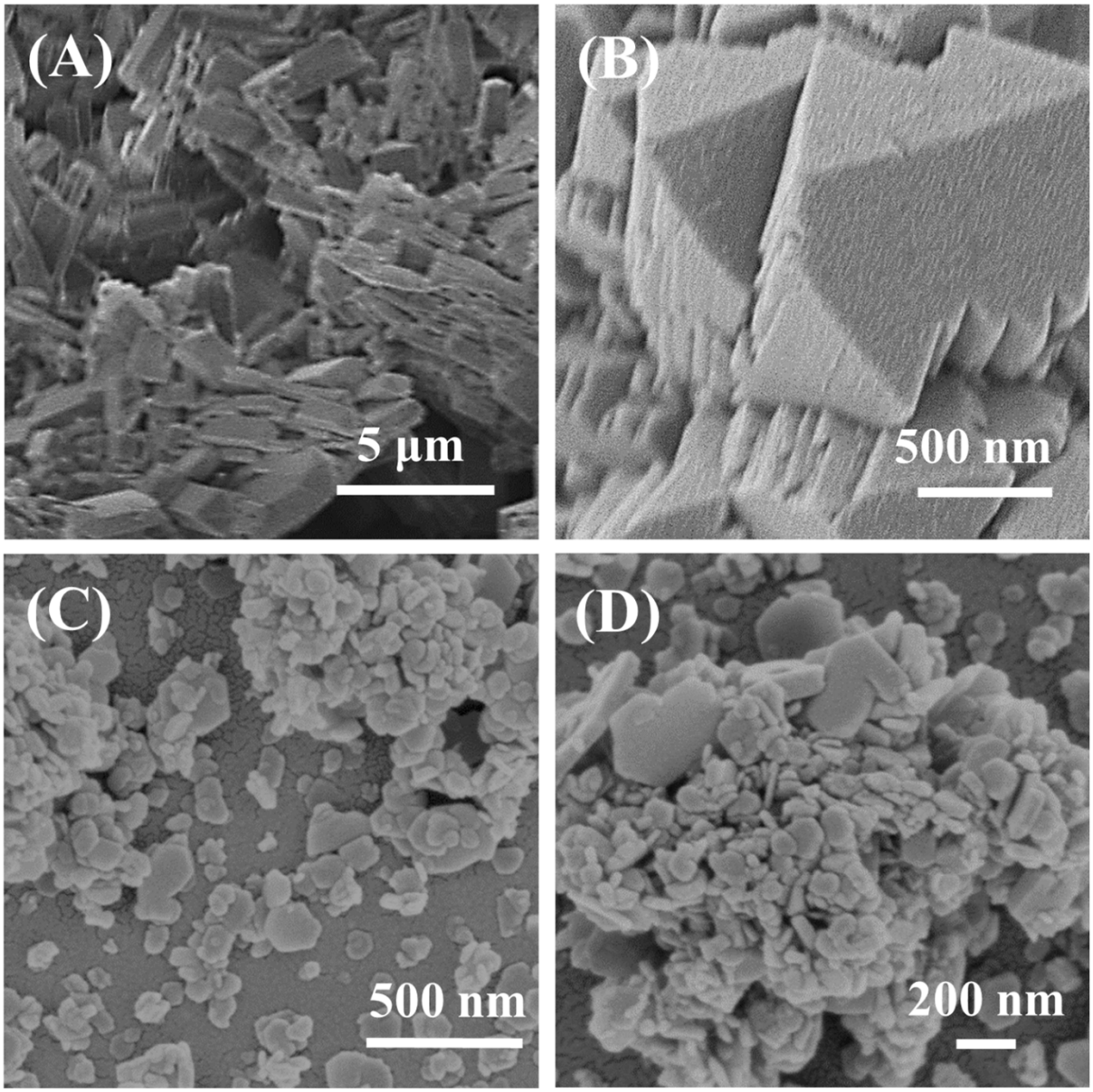

Fig. S3 SEM images of (A-B) CoC_2O_4 and (C-D) $Co(OH)_2$.

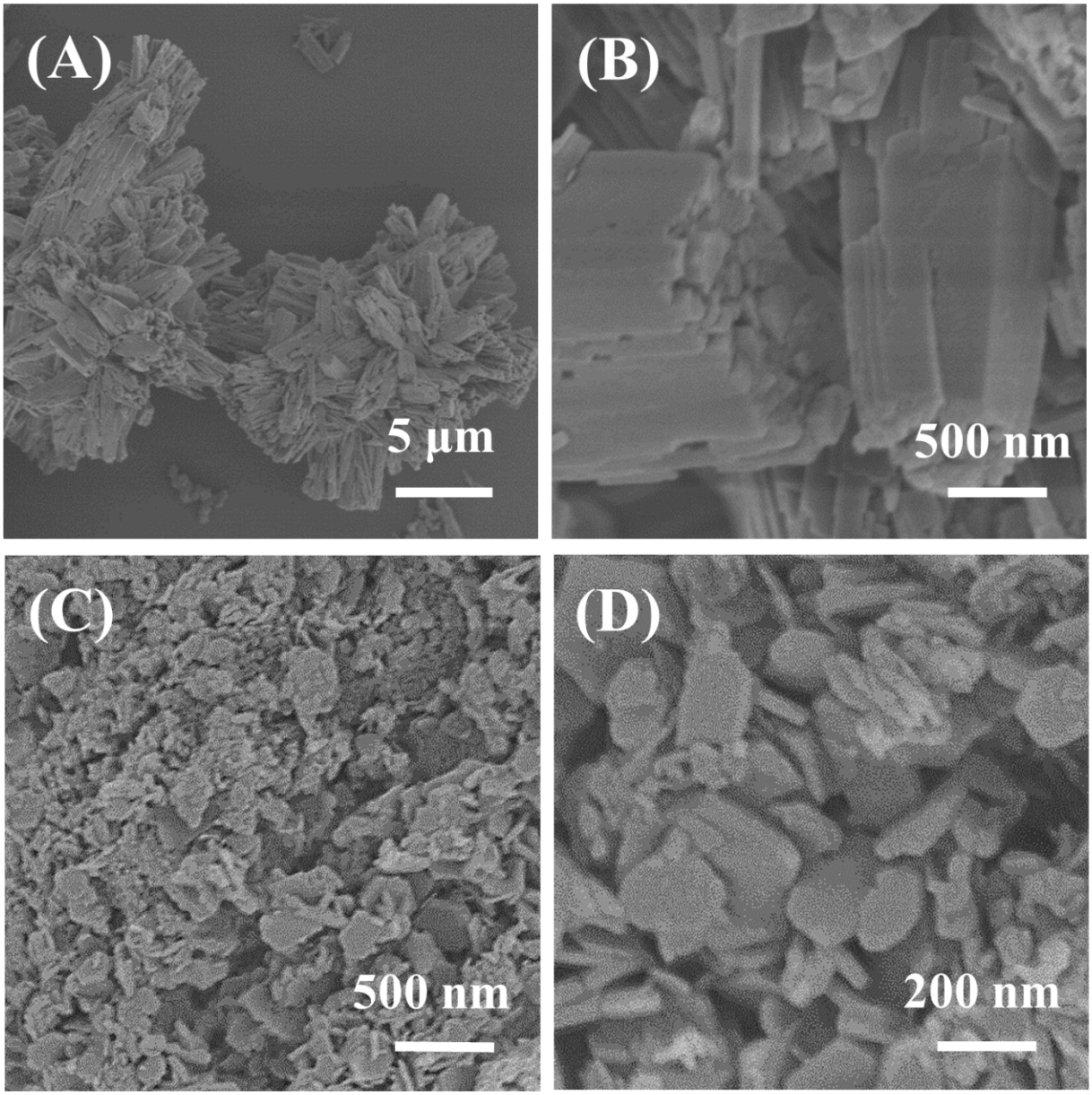

Fig. S4 SEM images of (A-B) Ru-CoC_2O_4-1 and (C-D) Ru-$Co(OH)_2$-1.

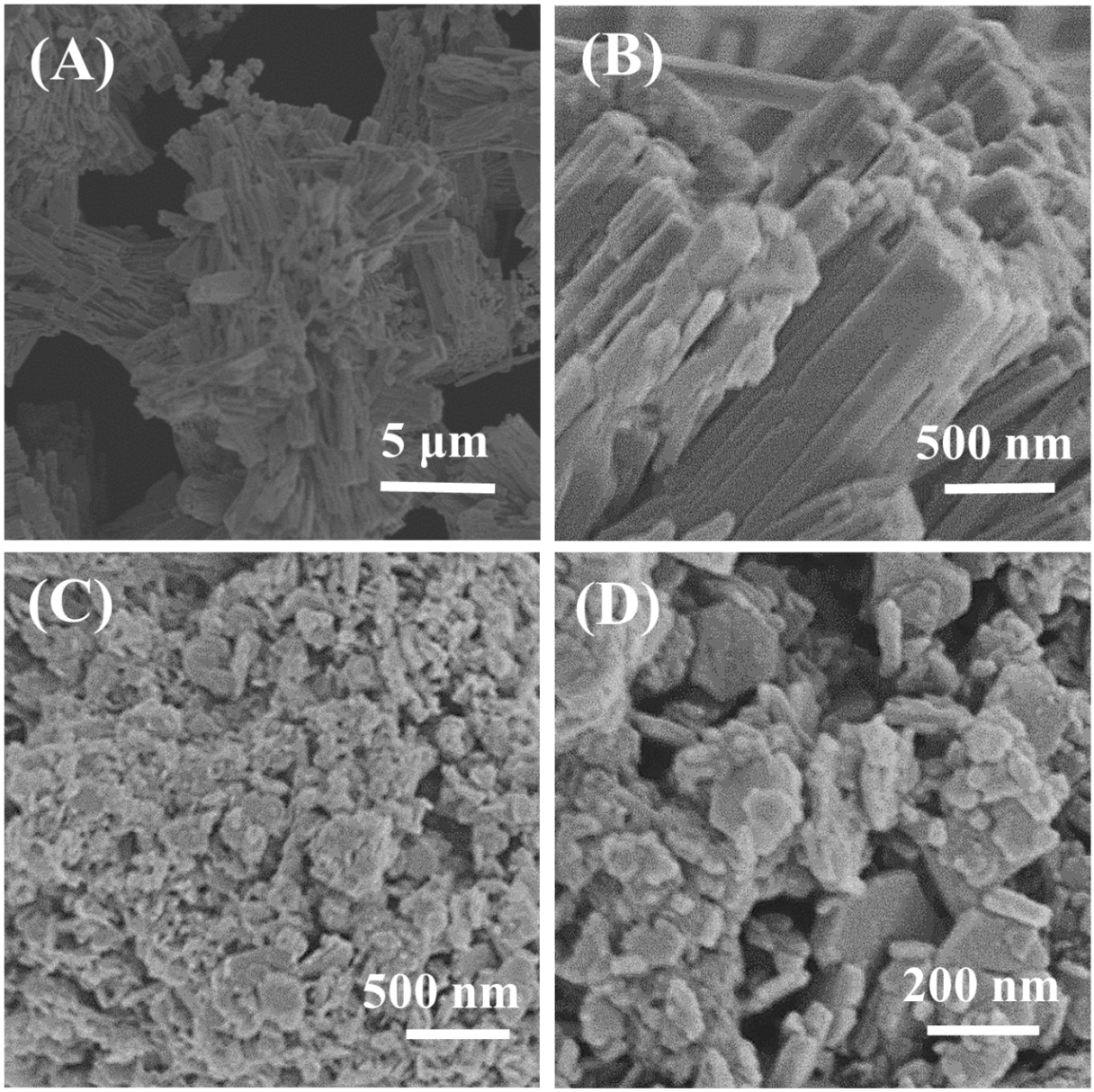

Fig. S5 SEM images of (A-B) Ru-CoC_2O_4-3 and (C-D) Ru-$Co(OH)_2$-3.

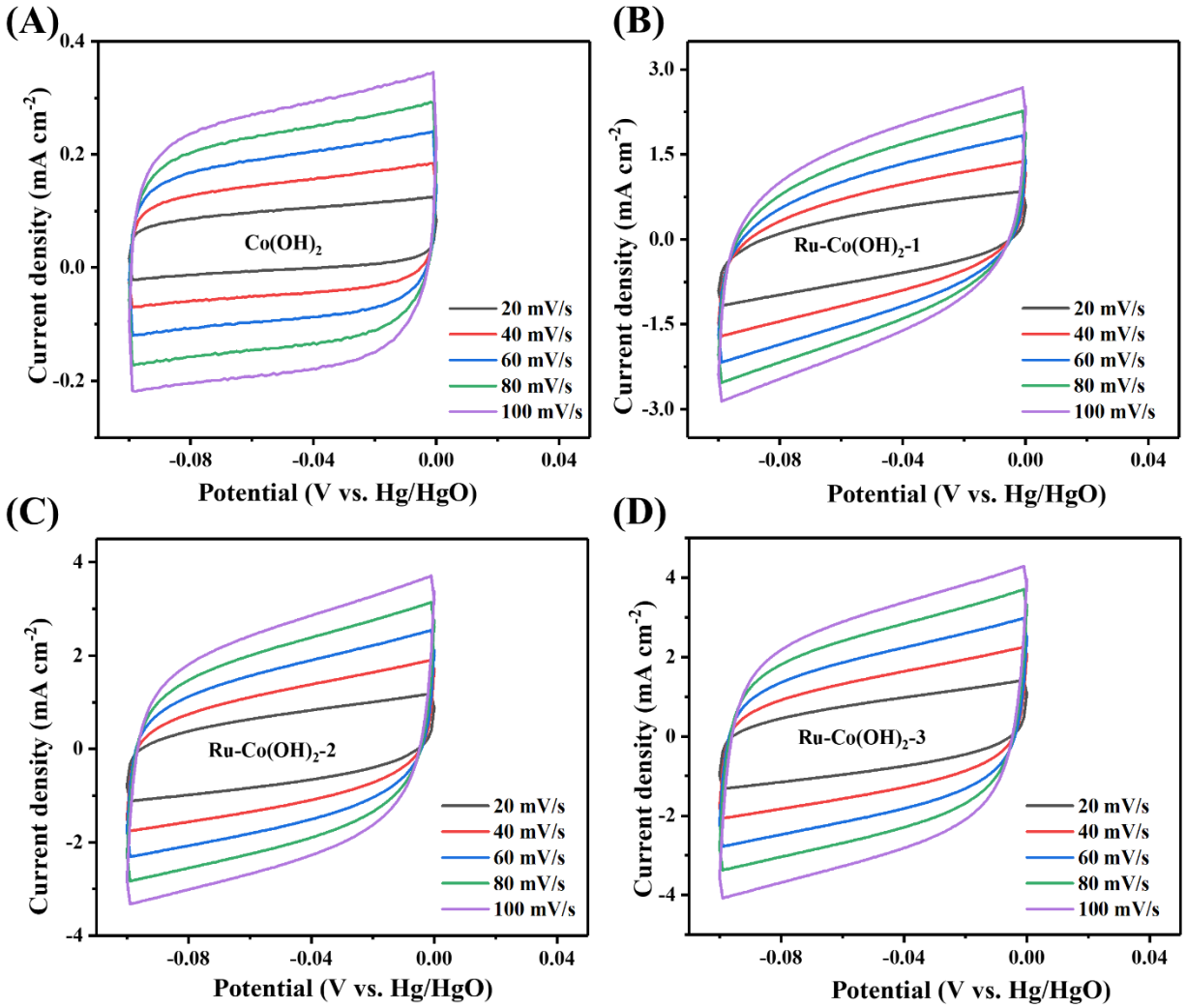

Fig. S6 Cyclic voltammetry profiles for (A) $Co(OH)_2$, (B) Ru-$Co(OH)_2$-1, (C) Ru-$Co(OH)_2$-2 and (D) Ru-$Co(OH)_2$-3 in 1.0 M KOH solution.

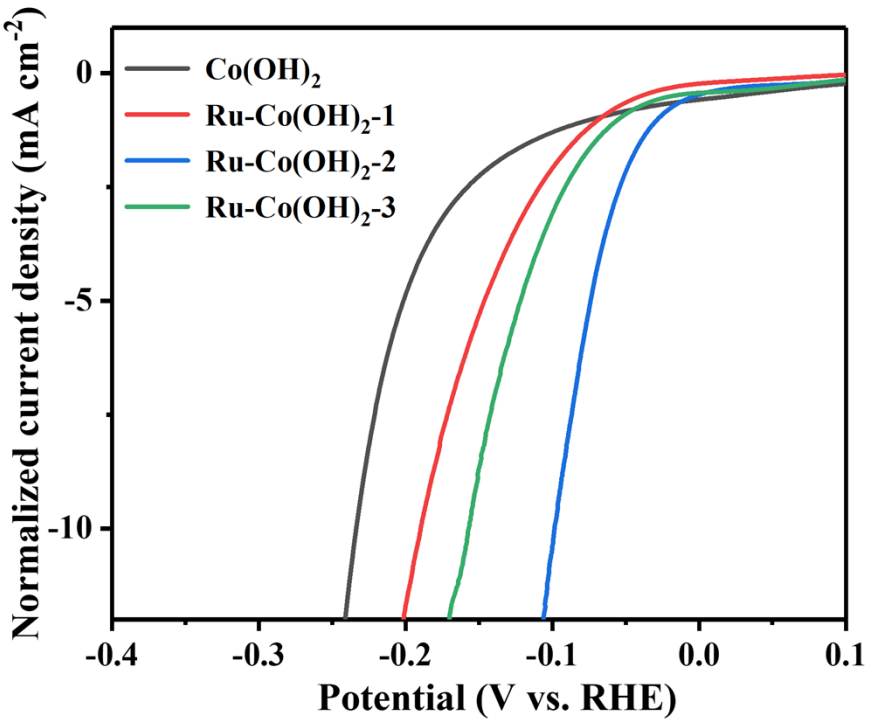

Fig. S7 ECSA-normalized LSV curves of the $Co(OH)_2$, Ru-$Co(OH)_2$-1, Ru-$Co(OH)_2$-2 and Ru-$Co(OH)_2$-3 in 1.0 M KOH solution.

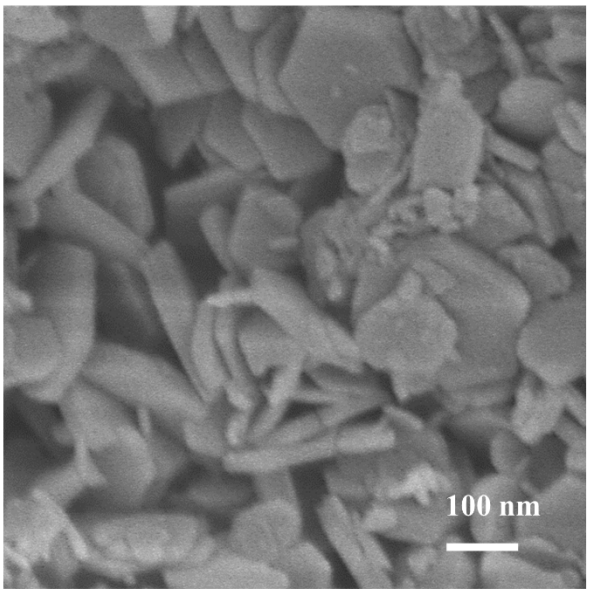

Fig. S8 SEM image of Ru-$Co(OH)_2$-2 after the HER performance testing.

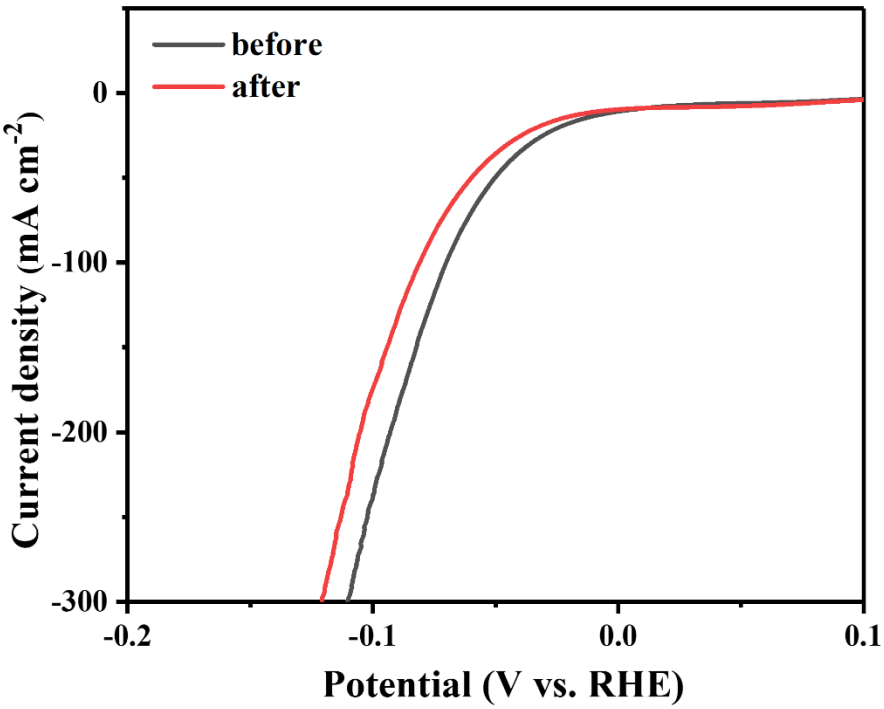

Fig. S9 LSV curves of the Ru-$Co(OH)_2$-2 before and after the stability test.

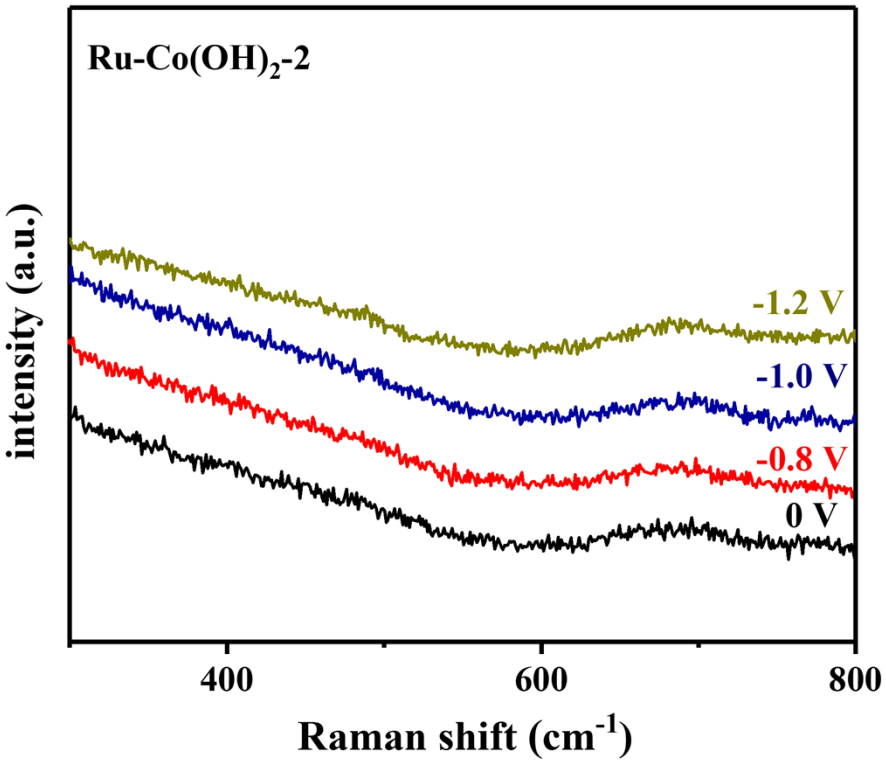

Figure S10 *In-situ* Raman spectra of Ru-$Co(OH)_2$-2 from -0.8 to -1.2 V vs. Hg/HgO.

Table S1. The Ru contents in different electrocatalysts measured by ICP-OES

Electrocatalysts	Ru Content (wt%)
Ru-$Co(OH)_2$-1	2.8
Ru-$Co(OH)_2$-2	5.1
Ru-$Co(OH)_2$-3	7.3

Table S2. Comparison of the HER performances of different Ru-based electrocatalysts in 1.0 M KOH

Sample	Overpotential (mV) at 30 mA cm^{-2}	Tafel slope ($mV\ dec^{-1}$)	References
Ru-$Co(OH)_2$-2	36	65	This work
Ru@C	160	96	1
$RuNi_1Co_1$@CMT	147	77	2
CoRu-O/A@HNC-2	140	73	3
Co/Se-MoS_2-NFs	110	70	4
B-CoP/CNT	90	80	5
RuCoP@CN	80	98	6
Ru/Co_3O_4 NWs	80	70	7
$Ru_{38}Pd_{34}Ni_{28}$/C	55	65	8
Co_5Ru_1@NCNT/PF	50	65	9
Pd–Ru@NG	50	73	10
Ru/CoO NRs	100	70	11
Ru-CMOP	80	96	12
Co NPs@Ru SAs/NC	98	84	13
Cu-RuS2/Ru	98	70	14
Ru/S-rGO-8	85	68	15
P-Ru-CoNi-LDH	65	69	16

References

1. M. Yang, T. Feng, Y. Chen, J. Liu, X. Zhao and B. Yang, *Appl. Catal. B*, 2020, **267**, 118657.
2. Y. Xue, Q. Yan, X. Bai, Y. Xu, X. Zhang, Y. Li, K. Zhu, K. Ye, J. Yan, D. Cao and G. Wang, *J. Colloid Interf. Sci*., 2022, **612**, 710-721.
3. G. Li, K. Zheng, W. Li, Y. He and C. Xu, *ACS Appl. Mater. Interfaces*, 2020, **12**, 51437-51447.
4. Z. Zheng, L. Yu, M. Gao, X. Chen, W. Zhou, C. Ma, L. Wu, J. Zhu, X. Meng, J. Hu, Y. Tu, S. Wu, J. Mao, Z. Tian and D. Deng, *Nat. Commun*., 2020, **11**, 3315.
5. E. Cao, Z. Chen, H. Wu, P. Yu, Y. Wang, F. Xiao, S. Chen, S. Du, Y. Xie, Y. Wu and Z. Ren, *Angew. Chem. Int. Ed.*, 2020, **59**, 4154-4160.

6. B. Yang, Y. Du, M. Shao, D. Bin, Q. Zhao, Y. Xu, B. Liu and H. Lu, *J. Colloid Interf. Sci*., 2022, **616**, 803-812.
7. Z. Liu, L. Zeng, J. Yu, L. Yang, J. Zhang, X. Zhang, F. Han, L. Zhao, X. Li, H. Liu and W. Zhou, *Nano Energy*, 2021, **85**, 105940.
8. D. Zhang, H. Zhao, B. Huang, B. Li, H. Li, Y. Han, Z. Wang, X. Wu, Y. Pan, Y. Sun, X. Sun, J. Lai and L. Wang, *ACS Cent. Sci*., 2019, **5**, 1991-1997.
9. J. Jiao, N.-N. Zhang, C. Zhang, N. Sun, Y. Pan, C. Chen, J. Li, M. Tan, R. Cui, Z. Shi, J. Zhang, H. Xiao and T. Lu, *Adv. Sci*., 2022, **9**, 2200010.
10. B. K. Barman, B. Sarkar and K. K. Nanda, *Chem. Commun*., 2019, **55**, 13928-13931.
11. J.-X. Guo, D.-Y. Yan, K.-W. Qiu, C. Mu, D. Jiao, J. Mao, H. Wang and T. Ling, *J. Energy Chem*., 2019, **37**, 143-147.
12. Q. Quan, Y. Zhang, F. Wang, X. Bu, W. Wang, Y. Meng, P. Xie, D. Chen, W. Wang, D. Li, C. Liu, S. Yip and J. C. Ho, *Nano Energy*, 2022, **101**, 107566.
13. H. Zhang, H. Su, M. A. Soldatov, Y. Li, X. Zhao, M. Liu, W. Zhou, X. Zhang, X. Sun, Y. Xu, P. Yao, S. Wei and Q. Liu, *Small*, 2021, **17**, 2105231.
14. Q. Shen, C. Du, Q. Chen, J. Tang, B. Wang, X. Zhang and J. Chen, *Mater. Today Phys*., 2022, **23**, 100625.
15. X. Sun, X. Gao, J. Chen, X. Wang, H. Chang, B. Li, D. Song, J. Li, H. Li and N. Wang, *ACS Appl. Mater. Interfaces*, 2020, **12**, 48591-48597.
16. Q. Li, F. Huang, S. Li, H. Zhang and X.-Y. Yu, *Small*, 2022, **18**, 2104323.